

DEVELOPMENT OF AN EXPERIMENTAL TECHNIQUE FOR HIGH TEMPERATURE IMPINGEMENT STUDIES

Evan L. Martin*, Lesley M. Wright*, and Daniel C. Crites**

*Baylor University, Waco, Texas, USA 76798

**Honeywell Aerospace, Phoenix, Arizona, USA 85034

evan.martin09@gmail.com; lesley_wright@baylor.edu

Keywords: gas turbine, impingement, heat transfer

Abstract

Modern gas turbine engines commonly operate at temperatures above the melting point of the turbine's blades and vanes. Internal and external cooling of the blades is required for sustained operation and prolonged engine life. Jet impingement, an aggressive form of cooling, is typically used in the airfoil leading edge which is exposed to extreme heat loads. Temperature differences between the cooling jets and blade walls can exceed 1000°F (556°C) in gas turbine engines. Frequently, jet impingement experimentation is performed at significantly lower temperature differences on the order of 60°F (33.3°C). The current experimental investigation attempts to bridge the gap between low temperature impingement studies and realistic turbine conditions. Using a transient technique, the lumped capacitance analysis, average Nusselt numbers are obtained from a row of round jets impinging on a leading edge model. Aluminum plates imbedded in a cylindrical target surface act as the lumped capacitance masses from which average Nusselt numbers can be obtained. The geometry of the impingement configuration is fixed at $\ell/d = 4$, $s/d = 4$, and $D/d = 5.5$. The jet Reynolds number and jet-to-target surface temperature difference range from 5,000 - 20,000 and 60°F - 400°F (33.3°C - 222°C), respectively. Heat transfer results are compared to existing leading edge impingement correlations. Over the range of temperatures considered in this investigation, the measured Nusselt numbers compare favorably to those predicted by existing correlations derived from low temperature experiments. Although lower than actual gas turbine engines, the temperature differences

investigated in this study represent an advance in impingement cooling research.

Nomenclature

A_s	=	surface area
Bi	=	Biot number
C_1, C_2	=	constants
c	=	specific heat capacity
D	=	diameter of cylindrical target surface
d	=	diameter of jet
E_{st}	=	energy storage
h	=	heat transfer coefficient
k	=	thermal conductivity of a solid
k_f	=	thermal conductivity of a fluid
k_{teflon}	=	thermal conductivity of Teflon PTFE
L	=	length of aluminum plate
L_c	=	characteristic length
ℓ	=	distance between jet plate and target surface
m	=	mass
Nu	=	Nusselt number
Q_{loss}	=	energy loss
Re_{jet}	=	$V_{jet} d / \nu_{jet}$, jet Reynolds number
r_1, r_2, r_3	=	radii
s	=	center-to-center distance between jets
T_∞	=	bulk fluid temperature
T_i	=	initial temperature
T_{jet}	=	jet temperature
T_{mass}	=	temperature of a mass
T_{plate}	=	average temperature of an aluminum plate
t	=	time
V_{jet}	=	velocity of jet at exit plane
ΔT	=	temperature difference
ν_{jet}	=	kinematic viscosity of jet

1 Introduction

Gas turbine engines literally 'power' the global economy and militaries around the world. They are crucial for power generation and

provide the necessary propulsion for military and passenger aircraft, ships, and even tanks. In the post-World War II era, gas turbine designers have sought to increase the overall thermal efficiency resulting in fuel savings and more power. A higher turbine inlet temperature directly boosts the thermal efficiency of a gas turbine engine. In modern engines, turbine inlet temperatures can surpass 3000°F (1649°C) whereas the turbine's blade and vanes may melt between 2000°F (1093°C) and 2600°F (1427°C). In order for the airfoils to withstand these extreme temperatures and to extend the service life of these engines, active cooling techniques are required.

Turbine airfoil cooling is accomplished through a combination of external and internal cooling. External cooling, referred to as film cooling, primarily consists of ejecting coolant through small holes distributed over the airfoil's surface. A buffer layer, or film, is created on the surface protecting the blade/vane from the hot gases exiting the combustor. On the other hand, the fundamental goal of internal cooling is to remove heat from the airfoil walls by circulating coolant through interior passages as illustrated in Fig. 1. A variety of methods are utilized to augment the heat transfer in these channels including ribs, dimples, and pin fins. Perhaps the most aggressive form of internal cooling is jet impingement. Impinging jets are typically used in the airfoil leading edge where stagnating combustion gases create extreme heat loads. Jet impingement can also be found throughout the midchord region of first-stage vanes as these airfoils experience the brunt of the intensely hot gases exiting the combustor.

Jet impingement investigations over the past 50 years have characterized many geometrical and flow parameters affecting impingement heat transfer on both leading edge (cylindrical target surface) and midchord region (flat target surface) models. However, many impingement studies are performed at jet-to-target surface temperature differences of approximately 100°F (55.6°C) or less. The coolant-to-airfoil wall temperature differences in modern gas turbine engines can approach 1000°F (556°C). As a result, there is a need to relate low temperature impingement

experimentation to realistic turbine operating conditions. For the sake of brevity, the majority of the literature reviewed pertains to leading edge or curved target surface impingement.

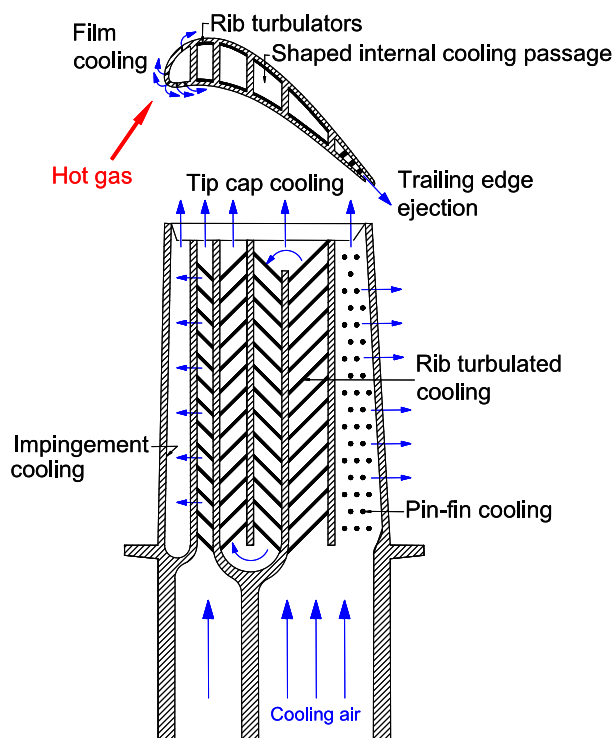


Fig. 1. Typical internal cooling scheme for a turbine blade [1].

Both steady state and transient experimental techniques are frequently employed to investigate jet impingement heat transfer. However, one technique may be more conducive to finding accurate heat transfer distributions on the target surface depending on the goals of the study and the available experimental apparatus. Yamashita [2], Jenkins [3], and Baltzer [4] studied a single row of round jets and a slot jet impinging on a concave target surface. An aluminum block encased in balsa wood formed the instrumented section of the curved target surface. Using a lumped capacitance technique, the aluminum block was heated to an initial temperature and then transiently cooled with room temperature air jets. Only one, average heat transfer coefficient could be obtained for temperature differences between the jet air and aluminum (initial temperature) of approximately 80°F (26.7°C) to 100°F (37.8°C). The results from these authors

DEVELOPMENT OF AN EXPERIMENTAL TECHNIQUE FOR HIGH TEMPERATURE IMPINGEMENT STUDIES

were compiled and summarized in two publications by Metzger et al. [5, 6]. Chupp et al. [7] performed a fundamental, parametric study of a single row of round jets impinging on a scale model of the leading edge. The cylindrical target surface was outfitted with nine parallel platinum strips each providing an average heat transfer coefficient. During the steady state testing, room temperature air impinged on the heated platinum strips achieving a temperature difference of about 60°F (33.3°C). The authors correlated the heat transfer results to encompass the effects of jet-to-target surface spacing, jet-to-jet spacing, and relative target surface curvature valid between jet Reynolds numbers of 3000 and 15000. Utilizing a fundamental copper plate method, Tabakoff and Clevenger [8] investigated slot jets, a single row of jets, and multiple rows of jets impinging on a cylindrical target surface. Five copper plates, individually heated by strip heaters, each provided an average heat transfer coefficient during steady state testing. The plates were maintained at 200°F (93.3°C) during testing while the jets were supplied with room temperature air ($\approx 70^\circ\text{F}$ or 21.1°C). Hrycak [9] distributed 21 cylindrical calorimeters over a curved target surface subject to a line of impinging jets. The calorimeters were constructed from stainless steel and heated with steam or electrical heaters from behind. A steady state heat transfer coefficient was calculated for each calorimeter using the temperature gradient measured by two thermocouples imbedded at two known locations in the stainless steel.

In the past two decades, several researchers have reported more resolved heat transfer distributions on concave target surfaces in the presence of jet impingement. Bunker and Metzger [10, 11] studied the effect of target surface sharpness on leading edge jet impingement. Local heat transfer coefficients were obtained by analyzing the melting patterns of coatings sprayed on the target surface. The coatings melted at approximately 110°F (43.3°C) under the influence of hot impinging jets. A steady state liquid crystal technique was performed by Lee et al. [12] to provide highly resolved heat transfer distributions for a single

impinging jet. An electrically heated thin gold film underneath the liquid crystal paint ensured a uniform heat flux condition over the entire concave target surface. The dependence of impingement heat transfer on jet Reynolds number was explored between Reynolds numbers of 11000 and 50000. Fénot et al. [13, 14] explored jet impingement on both a flat and a cylindrical target surface using steady state infrared thermography. In the flat plate study, the jet air was heated to a maximum temperature of 284°F (140°C) with an ambient temperature of about 70°F (21.1°C). The part of the study incorporating a concave target surface achieved temperature differences between the jet and ambient air up to 70°F (38.9°C). The jet Reynolds numbers ranged from 10000-23000. Since 2001, Taslim et al. [15-20] have exhaustively explored the effects of film cooling extraction and surface roughness relating to round and racetrack jet impingement. However, the authors employed a fundamental copper plate technique providing overall heat transfer coefficients rather than detailed distributions. Throughout the steady state testing, the temperature difference between the jets and heated copper plate was maintained at a constant 45°F (25°C).

Generally, the researchers described above observed similar trends regarding impingement heat transfer in the leading edge. An increase in jet Reynolds number enhances overall heat transfer. Moving the jets closer to the target surface and reducing the spacing between jets serve to independently increase heat transfer. Finally, broadening the diameter of the target surface as compared to the jet diameter slightly augments heat transfer levels in the leading edge.

The current study presents the development of a technique to measure impingement heat transfer at large temperature differences. A row of hot, round jets will impinge on a large-scale model of an airfoil leading edge. A temperature difference of 400°F (222°C) between the jets and target surface will be achieved at the beginning of a transient test. Validation cases will be performed at much lower temperature differences of approximately 60°F (33.3°C). Average stagnation Nusselt numbers will be

obtained using a transient lumped capacitance analysis. The reported values will be compared against the correlation developed by Chupp et al. [7] over a jet Reynolds number range of 5000 to 20000. The impingement geometry will be fixed at a jet-to-target surface spacing (ℓ/d) of four, jet-to-jet spacing (s/d) of four, and relative target surface curvature ratio (D/d) of 5.5.

2 Experimental Facilities

A specially-designed high temperature impingement rig is utilized for the present study. The design is based on scaled up model of the experimental apparatus used by Chupp et al. [7]. Compressed air is supplied to the impingement rig through a piping network consisting of two moisture separators, a regulator, and a one inch (0.0254 m) ASME square-edged orifice meter (Fig. 2). The mass flow rate through the system is determined based on the desired jet Reynolds number. An expression developed by Leary and Tsai [21] for mass flow rate through a square-edged orifice allows for the correct settings of upstream pressure and pressure drop across the orifice to achieve the desired Reynolds number at the jet. An oil manometer with a five inch (0.127 m) range measures the pressure drop at the orifice meter. The compressed air then flows through a pipe heater and a pneumatic three way valve. The three way valve either directs the heated air to an exhaust chimney to be vented to the atmosphere or diverts it into the impingement rig for testing purposes.

The impingement facility consists of three main components: the plenum, the carriage, and the chimney (Fig. 3a). From the three way valve, hot air is supplied to the plenum which promotes uniform flow and houses the exchangeable jet plate. The jet plates are constructed from 0.313 inch (0.008 m) steel and measure 16.875 inches (0.427 m) in length and 0.960 inches (0.024 m) in width. For the present study, the jet diameter, d , is fixed at 0.316 inches (0.008 m) with a center-to-center jet spacing, s , of 1.25 inches (0.032 m) (Fig. 3b). The resulting non-dimensional jet-to-jet

spacing, s/d , is four. Due to mass flow rate limitations through the pipe heater, only seven holes (or jets) are present on the jet plate. However, enough jets are maintained on the jet plate so that four jet periods impinge on the instrumented section of the target surface. Two J-type thermocouples measure the air temperature of the two outermost jets on the jet plate. Opposite the plenum and jet plate is the concave target surface supported by the carriage. The carriage allows for movement of the target surface either closer or further from the exit plane of the jets. As in Fig. 3c, the distance between the apex of the target surface and the jet plate is set to be approximately 1.25 inches (0.032 m) ($\ell/d = 4$). After impingement on the target surface, the spent air flows around the plenum and out through the chimney. The chimney's purpose is to promote the mixing of ambient air with the heated air exiting the impingement rig so that the mixed air departs the chimney at a safe and manageable temperature.

As illustrated in Fig. 4a, the target surface is comprised of three individual sections made of Virgin Electrical Grade Teflon polytetrafluoroethylene (PTFE). Teflon PTFE is a high performance plastic that can operate in temperatures up to 500°F (260°C). The two outer 'guard' surfaces measure 7.188 inches (0.183 m) long and five inches (0.127 m) across the face with a 1.75 inch (0.044 m) diameter half cylinder ($D/d = 5.5$) running down the center (Fig. 3c). The instrumented (center) section measures 5.5 inches (0.140 m) long and is identical in all other dimensions to the two guard surfaces. These three sections slide successively into a steel housing and held in place by means of a small wedge. The steel housing assembly is easily inserted into the carriage during transient testing.

The center section of the impingement surface accommodates the instrumentation necessary to provide the desired impingement heat transfer data (Fig. 4b). The apex of the curvature is outfitted with three 6061 aluminum plates each measuring five inches (0.127 m) long and isolated by 0.013 inch (0.0003 m) thick Teflon PTFE strips. For each plate, the chord length of the exposed surface is 0.368

DEVELOPMENT OF AN EXPERIMENTAL TECHNIQUE FOR HIGH TEMPERATURE IMPINGEMENT STUDIES

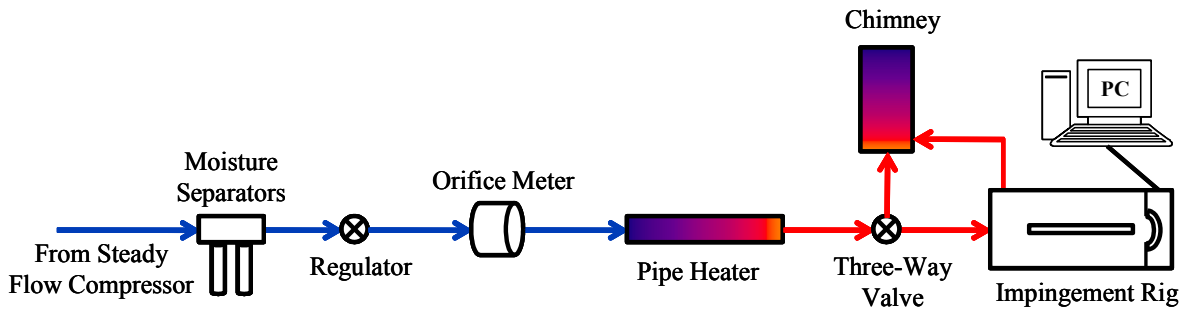


Fig. 2. Diagram of flow path and experimental facility.

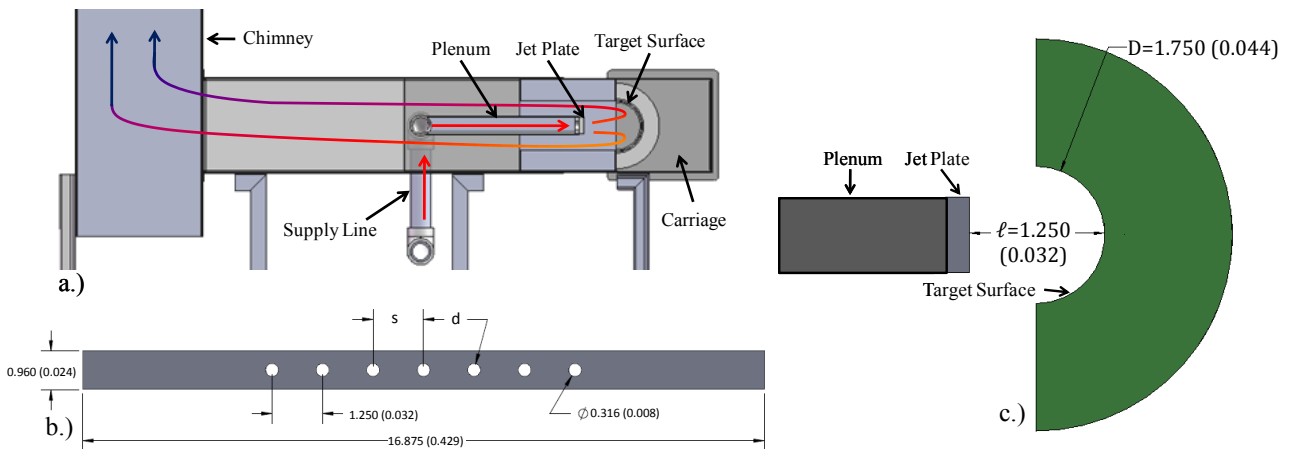


Fig. 3. Overview of high temperature impingement rig. a.)Flow path of air through impingement rig b.)Dimensioned jet plate in inches (m) c.)Relative position of jet plate and target surface in inches (m).

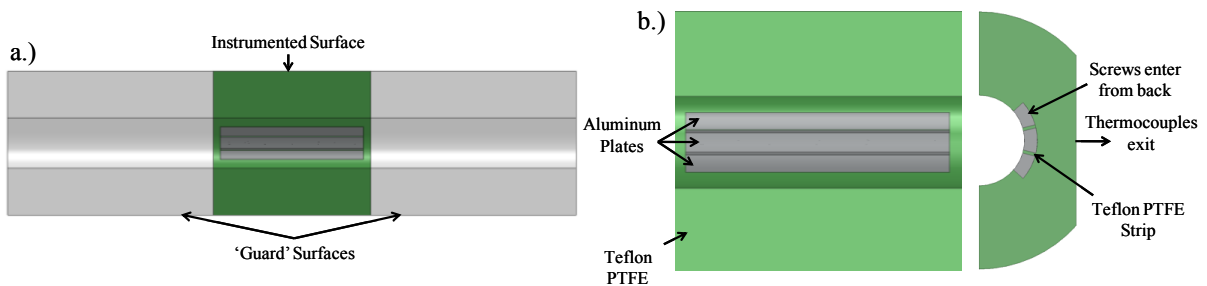


Fig. 4. Target surface overview. a.)Top view of three-piece target surface b.)Instrumented surface

inches (0.009 m) with a plate thickness of 0.25 inches (0.006 m). The chord length was established according to the width of the platinum strips employed by Chupp et al. [7]; scaled up to be consistent with the current impingement rig. The plate thickness was selected to satisfy the Biot number condition of the lumped capacitance method (discussed in the next section). The middle plate and one side plate are each instrumented with five J-type thermocouples. The thermocouples are soldered 0.125 inches (0.003 m) from the impingement surface and distributed along the length of the plates. An average of the five thermocouples in each plate is taken to provide an overall plate temperature at a given time.

Data acquisition is performed through National Instruments hardware coupled with National Instrument’s LabVIEW software. Before transient testing begins, the two jet thermocouples are continually monitored as the rig is preheated to approximately 130°F (54.4°C) or 470°F (243.3°C) depending on the temperature difference required. Once the temperature within the rig is steady, hot air is diverted to the chimney and the target surface is loaded into the carriage. Immediately, the heated air is directed back through the jet plate to impinge on the target surface and the jet and plate temperatures are recorded through time. As illustrated in Fig. 5, a near step change in jet temperature is achieved at the beginning of the test due to preheating the impingement rig. After testing is complete, a cool down period is required before another test can be completed. The time and temperature data gathered during testing facilitates the calculation of an average heat transfer coefficient for the middle aluminum plate by means of the lumped capacitance method.

3 Lumped Capacitance Technique

3.1 General Theory

The lumped capacitance method is a transient technique employed to solve for heat transfer coefficients in time dependent heat transfer problems. In general, this approach

pertains to a high conductivity mass that experiences a sudden temperature change in its surrounding environment (Fig. 6). The temperature throughout the mass is initially uniform and constant. A change in the temperature at the boundary of the mass initiates a change in the temperature of the mass. The temperature of the mass uniformly varies with time until an equilibrium state is reached. If the temperature of the mass as a function of time is known, then the lumped capacitance method can be applied to solve for the average heat transfer coefficient at the surface.

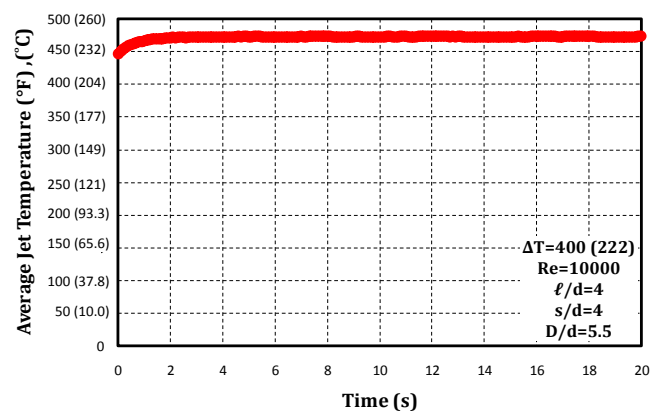


Fig. 5. Transient plot of the average jet temperature.

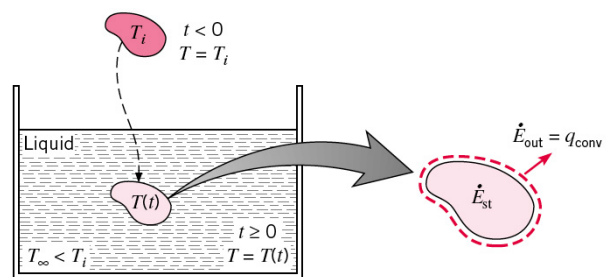


Fig. 6. Example of lumped capacitance heat transfer problem [22].

The primary assumption in the lumped capacitance method is that the spatial temperature profile in the mass is constant, meaning that temperature gradients within the mass are negligible. Hence, the temperature of the mass may change with time but the temperature throughout the mass must be uniform at a given time. Although this assumption is physically impossible, many problems come close to attaining this characteristic. For example, highly conductive

metals, like copper or aluminum, allow heat to diffuse quickly so that near constant internal temperature profiles can be achieved. To check the assumption's validity, the Biot number, Bi , must be calculated using the expression:

$$Bi = \frac{hL_c}{k} \quad (1)$$

where h is the heat transfer coefficient, L_c is a characteristic length, and k is the thermal conductivity of the mass. The Biot number describes the ratio of the object's internal resistance to heat flow to the thermal resistance across a fluid boundary layer. To apply lumped capacitance, the following condition must be satisfied:

$$Bi < 0.1 \quad (2)$$

A simple interpretation of this condition is that the temperature variation within the mass must be less than ten percent of the temperature difference between the surface and the fluid. If this condition is satisfied, temperature gradients in the mass can be neglected and the lumped capacitance method is valid to implement. Another key assumption is that a step change occurs in the temperature of the fluid surrounding the mass. This allows for a time invariant boundary condition at the fluid-to-mass interface.

To develop the lumped capacitance method, a transient energy balance must be performed between the mass and the fluid. The heat transfer rate at the fluid-to-mass interface is equated to the time rate of change of the internal energy within the mass resulting in:

$$-hA_s(T_\infty - T_{mass}(t)) = mc \frac{dT}{dt} \quad (3)$$

$$T_{mass}(t=0) = T_i \quad (4)$$

where A_s is the exposed surface area of the mass, T_∞ is the bulk fluid temperature, $T_{mass}(t)$ is the temperature of the mass as a function of time, m is the object's mass, c is specific heat capacity of the mass, and T_i is the uniform initial temperature of the mass. Equation (4) is an initial condition needed to solve the ordinary

differential equation in Eq. (3). The solution to the differential equation is determined to be:

$$T_{mass}(t) = T_\infty - \exp\left(-\frac{hA_s t}{mc}\right)(T_\infty - T_i) \quad (5)$$

where Eq. (5) can be rearranged to evaluate the heat transfer coefficient directly.

3.2 General Theory

The aluminum plates discussed in Section II act as lumped capacitance masses that are initially at room temperature ($\approx 70^\circ\text{F}$ or 21.1°C). At the start of a transient, the exposed aluminum surfaces are suddenly introduced to hot, impinging jets. The temperature of the plates steadily increases with time until the test ends. Throughout this heating process, the high thermal conductivity of the aluminum helps to ensure temperature uniformity throughout the plates. However, the Biot number needs to be calculated to verify the condition in Eq. (2) is satisfied. After substituting the thickness of the aluminum plates (0.25 inches or 0.003 m) for the characteristic length (L_c), a 'worst-case' Biot number is calculated to be 0.035. This result is almost an order of magnitude lower than the required 0.1 indicating the lumped capacitance method is valid for the present setup.

Updating and rearranging Eq. (5) to incorporate parameters unique to this high temperature impingement results in the following equation:

$$h = -\frac{mc}{A_s t} \ln\left(\frac{T_{jet} - T_{plate}(t)}{T_{jet} - T_i}\right) \quad (6)$$

where h is the average surface heat transfer coefficient, m is the mass of an aluminum plate, c is specific heat capacity of 6061 aluminum, A_s is the surface area of the plate exposed to the impinging fluid, T_{jet} is the jet temperature at the exit plane, $T_{plate}(t)$ is the average temperature of the plate, and T_i is the average, initial temperature of the aluminum plate. For purposes of comparison to other studies, a dimensionless heat transfer parameter, the Nusselt number (Nu), is calculated based on the heat transfer coefficient. The Nusselt number

compares the level of convective heat transfer to conductive heat transfer across a fluid/surface interface. A Nusselt number equal to one indicates a case of pure conduction (i.e. stagnant air in contact with a heated surface). On the other hand, a Nusselt number greater than one represents the relative heat transfer enhancement gained by the motion of the fluid. The Nusselt number is defined by the following expression:

$$Nu = \frac{hd}{k_f} \quad (7)$$

where d is the diameter of the jet and k is the thermal conductivity of the impinging air. The Nusselt number is, effectively, a scaled, non-dimensional heat transfer coefficient. Consequently, general trends are the same for both parameters. From this point forward, the heat transfer coefficient will be discussed in terms of the Nusselt number.

Equation (6) allows for the straightforward calculation of the heat transfer coefficient and consequent non-dimensional Nusselt number. However, a problem arises with the current target surface setup as it does not fit the framework of a fundamental lumped capacitance problem. Only one surface of the aluminum plates is exposed to the impinging fluid. As a result, conduction losses occur through the aluminum surfaces in contact with the Teflon support material. Theoretically, the Nusselt number is independent of time in transient testing. Thus, the experimental value of the Nusselt number could be taken at any point in time within a valid test. However, in this study, the Nusselt number rapidly increases to a maximum and then steadily decreases until the end of the data is reached. Fig. 7 illustrates the occurrence of the Nusselt number maximum and subsequent decrease in Nusselt number through time in the initial stage of a typical transient test. The steady decrease of the Nusselt number is due to conduction losses from the aluminum plates through the Teflon solid. In a fundamental lumped capacitance problem, the entire surface area of the solid is exposed to the convective fluid and conduction losses are non-existent. Fortunately, a reasonable Nusselt

number is still obtained in spite of the heat losses incurred throughout the impingement test. The Nusselt number maximum occurs within 1.5 to 3 seconds of the start of a given test before the conduction losses from the aluminum plates become significant. As a result, the experimental Nusselt number values reported in the next section are the ‘peaks’ of these Nusselt number curves as exhibited in Fig. 7.

The short times at which the Nusselt number culminates in a maximum value leads to high experimental uncertainties. Early in a test, the aluminum plates experience little temperature increase over the initial temperature. Therefore, the accuracy of the J-type thermocouples is the primary factor influencing the high uncertainties observed in this study. For a high Nusselt number (≈ 90), the experimental uncertainty is approximately 25% using the methods of Kline and McClintock [23].

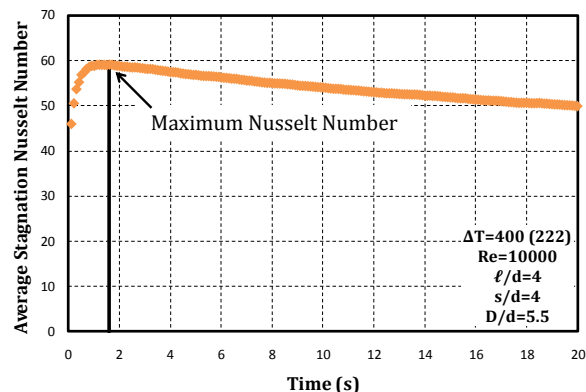


Fig. 7. Degradation of Nusselt number through time and location of maximum Nusselt number.

4 Results and Discussion

4.1 Nusselt Number Results

For the purposes of the current study, only Nusselt number results from the middle plate (stagnation region) are reported. As briefly mentioned previously, Chupp et al. [7] developed a correlation to predict an average Nusselt number along a stagnation strip located at the apex of the target surface. The correlation incorporates non-dimensional flow and

geometrical parameters to aid in determining jet impingement heat transfer for various layouts and schemes. The results from the middle aluminum plate of this study can be directly compared to the Chupp et al. [7] correlation. Figure 8 presents high temperature ($\Delta T = 400^\circ\text{F}$ or 222.2°C) and low temperature ($\Delta T = 60^\circ\text{F}$ or 33.3°C) experimental data for a fixed geometry ($\ell/d = 4$, $s/d = 4$, and $D/d = 5.5$) as compared to the correlation. The data are plotted for three jet Reynolds numbers: 5000, 10000, and 20000. It should be noted that the dashed, black line indicates data from the correlation that lies outside the prescribed limitations of Chupp et al. [7] ($3000 \leq Re_{jet} \leq 15000$).

Overall, the high and low temperature experimental data agree well with the Chupp et al. [7] correlation. The experimental markers at $Re_{jet} = 5000$ and $Re_{jet} = 10000$ lie directly on the correlation line. The percent variation at these two Reynolds numbers is less than 2.5%. At $Re_{jet} = 20000$, some variation is noticeable between the experimental data and the correlation as well as between the markers themselves. However, only 8.6% difference and 6.3% difference exists between the predicted Nusselt numbers and the high and low temperature data, respectively. Also, at $Re_{jet} = 20000$, the correlation is outside the limits defined by the authors. Consequently, the accuracy of the correlation at higher Reynolds numbers may be compromised. Further investigation is required to fully characterize the accuracy of the correlation beyond its prescribed boundaries. The percent difference between the high and low temperature data points is 2.3% indicating close experimental agreement even at high Reynolds numbers.

Several important observations can be drawn from Fig. 8. First, the experimental technique outlined in the current study produces average Nusselt numbers that agree well with a previously published and respected leading edge impingement correlation. Despite the high uncertainty, reporting the maximum value of the average stagnation Nusselt number provided reasonable heat transfer results with no anomalies or unusual trends. Next, an increase of jet-to-target-surface temperature difference from 60°F (33.3°C) to 400°F (222°C) had a

negligible effect on average stagnation Nusselt numbers. Recall that Chupp et al. [7] investigated leading edge impingement at a temperature difference of approximately 60°F (33.3°C). Increasing the temperature difference nearly seven-fold indicated no significant degradation or enhancement of impingement Nusselt numbers. Although the Nusselt number is insensitive to temperature, the heat transfer coefficient does increase with increasing temperature difference. For commercial applications, it is crucial to correctly interpret the Nusselt number so that accurate heat transfer coefficients can be determined. Finally, the method of accounting for conduction losses by reporting the maximum Nusselt number value was apparently successful. However, quantitatively accounting for these losses is judicious and desirable. The following section outlines a proposed method to characterize conduction losses from the middle aluminum plate into the Teflon PTFE surface using a modified lumped capacitance analysis.

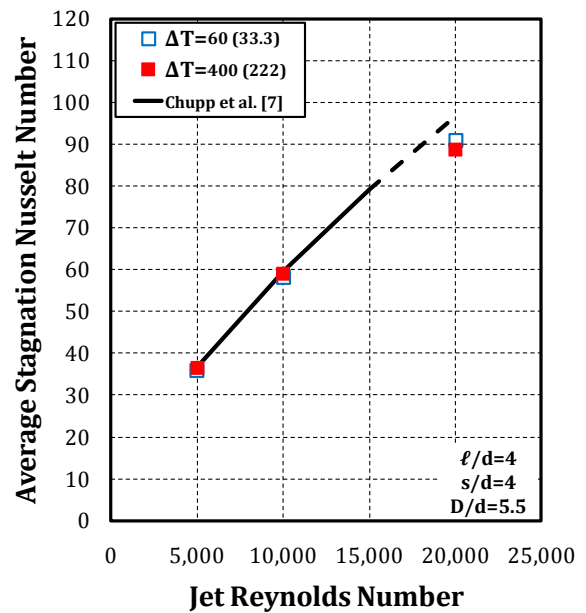


Fig. 8. Comparison of experimental data and the Chupp et al. [7] correlation.

4.2 Heat Loss Correction

Heat loss from the middle aluminum plate to the surrounding Teflon PTFE material can be treated as a traditional radial conduction problem. The rate of energy loss is expressed as

a temperature difference multiplied by the inverse of thermal resistance:

$$\dot{Q}_{loss}(t) = [T_{plate}(t) - T_i] \left[\frac{2\pi L k_{teflon}}{\ln\left(\frac{r_3}{r_2}\right)} \right] \quad (8)$$

where L is the length of an aluminum plate, k_{teflon} is the thermal conductivity of Teflon PTFE, and r_2 and r_3 are radii. Figure 9 graphically depicts the definition of r_2 and r_3 as well as the direction of energy flow through the target surface and assumed temperatures within the physical setup. Two assumptions are critical in the development of this energy loss term. The temperature at the aluminum-to-Teflon interface is the same as the temperature of the aluminum plate and the temperature of the backside of the Teflon remains at the initial temperature throughout the course of the test. This latter assumption is the most difficult to satisfy, particularly at high temperatures, as will be explained shortly. Applying the energy loss term in Eq. (8) to a revised energy balance forms the ordinary differential equation below:

$$mc \frac{dT}{dt} = hA_s (T_{jet} - T_{plate}(t)) + (T_{plate}(t) - T_i) \left[\frac{2\pi L k_{teflon}}{\ln\left(\frac{r_3}{r_2}\right)} \right] \quad (9)$$

After a moderate amount of algebra and calculus, a solution to the differential equation is of the form:

$$\frac{T_{plate}(t) - \frac{C_1 T_{jet} + C_2 T_i}{C_1 + C_2}}{T_i - \frac{C_1 T_{jet} + C_2 T_i}{C_1 + C_2}} = \exp(-(C_1 + C_2)t) \quad (10)$$

where

$$C_1 = \frac{hA_s}{mc} \quad (11)$$

$$C_2 = \left(\frac{2\pi L k_{teflon}}{mc \ln\left(\frac{r_3}{r_2}\right)} \right) \quad (12)$$

Unlike the general lumped capacitance method, this modified lumped capacitance analysis requires the heat transfer coefficient, h , to be solved numerically from Eq. (10).

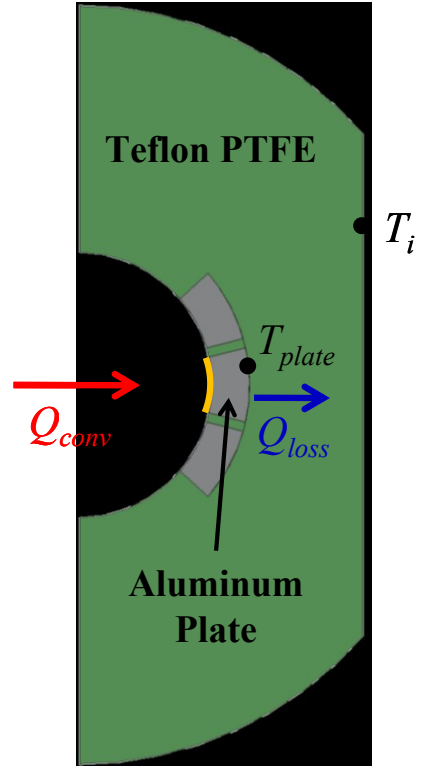


Fig. 9. Thermal circuit of heat loss through target surface.

Figure 10 presents the same data as Fig. 7 with the added comparison of heat-loss-corrected Nusselt numbers. Leading up to the occurrence of the maximum Nusselt number the uncorrected and corrected Nusselt number values are in close agreement. Following the location of the maximum Nusselt number, corrected values level off whereas the uncorrected values decrease through time. The corrected values correspond well to the reported maximum Nusselt number over the initial 20 seconds of the transient test. An increasing trend in the corrected Nusselt number is noticeable beginning at approximately 16 seconds. The authors partially attribute this to a violation of the assumption that the backside of the Teflon PTFE remains at T_i throughout the experimental

test. In reality, during a typical test, some heating occurs through the opposite side of the Teflon due to preheating the rig before testing. Alternatively, the middle plate is flanked by two other aluminum plates that also heat up during a test run. Only a thin strip of Teflon PTFE isolates the middle plate from the other two plates. As a test progresses, the middle plate may absorb heat conducting through the Teflon spacers from the other plates.

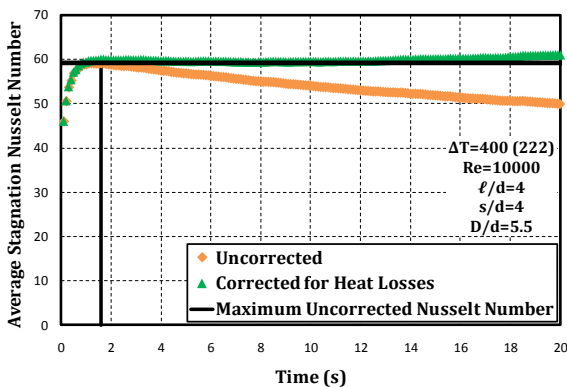


Fig. 10. Corrected Nusselt number values compared to uncorrected values through time.

In general, however, the development of a modified lumped capacitance analysis proved successful in quantitatively accounting for conduction losses. The corrected Nusselt number values indicate that the maximum uncorrected Nusselt number is a reasonable estimate of the actual impingement Nusselt number value.

5 Conclusions

High temperature jet impingement on a turbine blade leading edge model was successfully investigated using a transient lumped capacitance technique. Average Nusselt number results were compared and validated against the correlation developed by Chupp et al. [7]. Furthermore, the effect of high temperature differences was shown to be insignificant in the calculation of the Nusselt number. This finding is important for engine designers using impingement data taken from relatively low temperature experimentation. Specifically, the Chupp et al. [7] correlation can be expanded beyond the original 60°F (33.3°C)

difference up to 400°F (222°C) temperature differences. This provides a stepping stone to characterizing impingement heat transfer in actual turbine operating conditions. Finally, the conduction losses from the middle aluminum plate were accounted for by incorporating a radial conduction term into the general lumped capacitance analysis. An advantage to this method is that no additional temperature measurements were required to quantify the heat losses. Also, capturing the maximum uncorrected Nusselt number value in the early stages of a test proved to be a reasonable means to account for heat losses and report the average stagnation Nusselt number. Unfortunately, the lumped capacitance method can only supply average Nusselt number values. In the future, the development a method to provide more detailed Nusselt number distributions would be advantageous. The average Nusselt number in the stagnation region has been shown to be insensitive to increased temperature differences. However, detailed distributions may show a different trend in other areas of the curved target surface where jet-to-target surface interactions are less intense and more indirect.

Acknowledgments

The authors would like to thank Honeywell, Inc. for its generous financial support of this study and Mr. Dan Crites and Dr. Malak Malak for their continuous involvement and advice throughout this project.

References

- [1] Han, J. C. and Wright, L. M. *Enhanced internal cooling of turbine blades and vanes*. The Gas Turbine Handbook, DOE, Office of Fossil Energy, National Energy Technology Laboratory, 2006.
- [2] Yamashita, T. *Heat Transfer characteristics of air jets from straight line arrays of circular nozzles impinging on concave semicylindrical surfaces*. M.S. Thesis, Arizona State University, Tempe, AZ, 1967.
- [3] Jenkins, C. W. *Impingement cooling of concave surfaces with slot jets and single lines of circular jets*. M.S. Thesis, Arizona State University, Tempe, AZ, 1969.
- [4] Baltzer, R. T. *Effects of impingement surface curvature on heat transfer characteristics of*

- impinging air jets*. M.S. Thesis, Arizona State University, Tempe, AZ, 1970.
- [5] Metzger, D. E., Yamashita, T., Jenkins, C. W. Impingement cooling of concave surfaces with lines of circular air jets. *ASME Journal of Engineering for Power*, Vol. 91, No. 3, pp. 149-158, 1969.
- [6] Metzger, D. E., Baltzer, R. T., Jenkins, C. W. Impingement cooling performance in gas turbine airfoils including effects of leading edge sharpness. *ASME Journal of Engineering for Power*, Vol. 94, No. 3, pp. 219-225, 1972.
- [7] Chupp, R. E., Helms, D. E., McFadden, P. W., and Brown, T. R. Evaluation of internal heat transfer coefficients for impingement cooled turbine airfoils. *AIAA Journal of Aircraft*, Vol. 6, No. 3, pp. 203-208, 1969.
- [8] Tabakoff, W., and Clevenger, W. Gas turbine blade heat transfer augmentation by impingement of air jets having various configurations. *ASME Journal of Engineering for Power*, Vol. 94, No. 1, pp. 51-60, 1972.
- [9] Hrycak, P. Heat transfer from a row of impinging jets to concave cylindrical surfaces. *International Journal of Heat and Mass Transfer*, Vol. 24, pp. 407-419, 1981.
- [10] Bunker, R. S., and Metzger, D. E. Local heat transfer in internally cooled turbine airfoil leading edge regions: part I - impingement cooling without film coolant extraction. *ASME Journal of Turbomachinery*, Vol. 112, pp. 451-458, 1990.
- [11] Metzger, D. E., and Bunker, R. S. Local heat transfer in internally cooled turbine airfoil leading edge regions: part II - impingement cooling with film coolant extraction. *ASME Journal of Turbomachinery*, Vol. 112, pp. 459-466, 1990.
- [12] Lee, D. H., Chung, Y. S., and Won, S. Y. The effect of concave surface curvature on heat transfer from a fully developed round impinging jet. *International Journal of Heat and Mass Transfer*, Vol. 42, pp. 2489-2497, 1999.
- [13] Fénot, M., Vullierme, J. -J, and Dorignac, E. A heat transfer measurement of jet impingement with high injection temperature. *C. R. Mécanique*, Vol. 333, pp. 778-782, 2005.
- [14] Fénot, M., Dorignac, E., and Vullierme, J. -J. An experimental study on hot round jets impinging on a concave surface. *International Journal of Heat and Fluid Flow*, Vol. 29, pp. 945-956, 2008.
- [15] Taslim, M. E., Setayeshgar, L., and Spring, S. D. An experimental evaluation of advanced leading edge impingement cooling concepts. *ASME Journal of Turbomachinery*, Vol. 123, pp. 147-153, 2001.
- [16] Taslim, M. E., Pan, Y., and Spring, S. D. An experimental study of impingement on roughened airfoil leading edge walls with film holes. *ASME Journal of Turbomachinery*, Vol. 123, pp. 766-773, 2001.
- [17] Taslim, M. E., Pan, Y., and Bakhtari, K. Experimental racetrack shaped jet impingement on a roughened leading-edge wall with film holes. *Proceedings of 2002 IGTI International Gas Turbine Conference and Exposition*, ASME Paper No. GT-2002-30477, 2002.
- [18] Taslim, M. E., Bakhtari, K., and Liu, H. Experimental and numerical investigation of impingement on a rib-roughened leading-edge wall. *ASME Journal of Turbomachinery*, Vol. 125, pp. 682-691, 2003.
- [19] Taslim, M. E., and Khanicheh, A. Experimental and numerical study of impingement on an airfoil leading edge with and without showerhead and gill film holes. *ASME Journal of Turbomachinery*, Vol. 128, pp. 310-320, 2006.
- [20] Taslim, M. E., and Bethka, D. Experimental and numerical impingement heat transfer in an airfoil leading-edge cooling channel with cross-flow. *ASME Journal of Turbomachinery*, Vol. 131, pp. 1-7 (011021), 2009.
- [21] Leary, W. A., Tsai, D. H. *Metering of gases by means of the ASME square-edged orifice with Flange taps*. Sloan Laboratory for Automotive and Aircraft Engines, Massachusetts Institute of Technology, 1951.
- [22] Incropera, F. P., Dewitt, D. P. *Fundamentals of mass and heat transfer*. 5th ed., John Wiley & Sons, Inc., Hoboken, NJ, 2002.
- [23] Kline, S. J. and McClintock, F. A. Describing uncertainties in single-sample experiments. *Mechanical Engineering*, 75, pp. 3-8, 1953.

Copyright Statement

The authors confirm that they, and/or their company or organization, hold copyright on all of the original material included in this paper. The authors also confirm that they have obtained permission, from the copyright holder of any third party material included in this paper, to publish it as part of their paper. The authors confirm that they give permission, or have obtained permission from the copyright holder of this paper, for the publication and distribution of this paper as part of the ICAS2012 proceedings or as individual off-prints from the proceedings.